Journal of Material Cycles and Waste Management (2021) 23:1189–1200
https://doi.org/10.1007/s10163-021-01210-x

ORIGINAL ARTICLE

The effects of cement raw mix waste dust on thermal properties of ceramic wall tile bodies

Tuna Aydin[1]

Received: 26 December 2019 / Accepted: 5 March 2021 / Published online: 11 March 2021

Abstract

The recycling of industrial wastes has in recent years become a priority issue. The relevant work on reducing the adverse effects of industrial wastes is becoming more important. Farina (raw mix) is a crude mixture obtained by grinding the raw materials used in cement production. The oxides at a high rate ensure that the cement raw mix waste dust is a good source of raw material in ceramic wall tile body production. This study used 2%, 3%, 5% and 10% cement raw mix waste dust instead of calcite, which is used in a standard wall tile recipe. Another industrial waste, marble dust, was also used as a source of $CaCO_3$. The physical and mechanical properties of prepared samples such as firing shrinkage, dry and fired strength, and water absorption were examined. And firing behavior using a non-contact optical dilatometer was also studied. The study showed that the addition of cement waste raw mix dust improves physical and mechanical properties. Dry strength and bending strength increased as the amount of cement waste raw mix dust increase. Bulk density also increased with the addition of cement waste raw mix dust. Especially, 50% increase in dry strength was achieved with the addition of cement waste raw mix dust instead of calcite. The sintering rate (dy/dt) was negatively affected, and sintering slowed down when the higher amount of the addition cement waste raw mix dust. The study showed that cement waste raw mix waste dust and marble dust can be used as alternative raw materials for ceramic wall tiles up to 5 wt % instead of $CaCO_3$.

Keywords Waste recycling · Cement raw mix dust · Ceramic wall tile · Marble dust

Introduction

Cement as a hydraulic binder contains raw materials such as limestone, iron oxide, and clay mixture. Cement is a building material obtained by melting the raw material mixture at high temperature and then grinding it with the addition of some gypsum to the clinker obtained through the instant cooling process. Crushing, sieving, and grinding are pre-physical processes for all cement raw materials during the cement production process [1, 2]. The high levels of dust generated during these processes also result in environmental problems and cause health problems. Especially, the production of cement results in poor air quality. In cement industry, the environmental emissions include nitrogen oxides, carbon monoxide, carbon dioxide, sulfur dioxide, chlorides, and fluorides, smaller quantities of organic compounds, heavy metals, and grey dust [3, 4]. These gases and dust cause both environmental and health problems. It was known that 5–6% of all carbon dioxide greenhouse gases due to the cement production [4]. The cyclones, multi-cyclone, bag filter, and electro-filter are used as dust chambers, in the production process to hold these dusts. However, the recycling of these powders has not received sufficient study. The cement raw mix waste dust from dust chambers contains a high percentage of oxides, such as SiO_2, Al_2O_3, CaO, Fe_2O_3, MgO, Na_2O and K_2O, which may allow use in the ceramic industry. Ceramic wall tile bodies contain high amount of calcite. Especially with their high CaO content, cement raw mixture waste dust and marble dust can be used as an alternative raw material in ceramic wall tile production [1]. Previous studies have demonstrated the ability to use cement raw mix waste dust as an alternative raw material source in porcelain tile bodies [1]. In previous study, cement raw mix waste dust improved physical and mechanical properties of porcelain tile bodies [1]. Ceramic tile production can also use industrial wastes such as sanitaryware waste, fly

✉ Tuna Aydin
tunaaydin@kku.edu.tr

[1] Department of Metallurgy and Material Engineering, Faculty of Engineering, Kirikkale University, 71450 Kirikkale, Turkey

ash, blast furnace slags and, waste glass as an alternative raw material. Previous studies have shown that sanitaryware waste increased the bulk density and bending strength of ceramic wall tile bodies [5]. The addition of blast furnace slag provided high strength in ceramic wall tiles and sanitaryware bodies [6, 7]. Today, one of the most important issues of ceramic manufacturers is access to raw materials and raw material costs. With the recycling of cement raw mix waste dust (CRMD) and marble dust, this study will provide an alternative source of raw materials that is environmentally friendly. Today trends are moving towards the production of large format ceramic wall tiles. Dry strength is one of the most important technological parameter that determine their production efficiency. Because, ceramic wall tiles are characterized as high porosity and high water absorption. The high porosity results in a decrease in dry strength. In this case, it causes an increase in semi-finished product damage, loss of product and a decrease in production efficiency. In this study, the recycling of CRMD and marble dust in an industrial application and the increase in dry strengths are the most important aspects that distinguish this study from previous studies. The study used cement raw mixed dust, 2%, 3%, 5%, and 10% by weight, instead of calcite, which is used in a standard ceramic wall tile composition.

Materials and methods

Kaolin, clay, calcite, quartz, and sodium feldspar were used in a standard ceramic wall tile recipe. CRMD and marble dust were used as a source of CaO instead of calcite. Aslan Cement Co., Kocaeli, Turkey provided the cement raw mix waste dust. In this study, marble dust was used instead of calcite in all compositions. STD body contains kaolin, clay, quartz, sodium feldspar, and calcite. RMD1 body is composed of kaolin, clay, quartz, sodium feldspar, CRMD, and marble dust. CRMD and marble dust were used in RMD1 in a ratio of 2% and 9%, respectively. RMD2 body contains CRMD and marble dust in a ratio of 3% and 8%, respectively. CRMD and marble dust were used in RMD3 body in a ratio of 5% and 6%, respectively. In RMD4 body, CRMD and marble dust were used in a ratio of 10% and 1%, respectively. After the grinding process, the slurry was dried in an oven at 110 °C for 24 h. The dry powders were made into granules ready for compression by providing moisture at 5–6%. The granules were shaped with a uniaxial dry press at a pressure of 280 kg/cm^2 to a size of 50 mm × 100 mm. The green bodies were then fired at 1130 °C under laboratory conditions. The sintering behavior was analyzed using non-contact optical dilatometer with heating rates of 10 °C min^{-1} (MISURA ODHT HSM 1600/80, Ceramic Research Centre, Turkey). The crystalline phases were detected with an X-ray diffractometer (Rigaku Rint, Ceramic Research Centre, Turkey) using a copper tube (Cu Kα radiation) in a 2θ angle interval from 5° to 70° with a 0.02° step. Tg–DTA analyses were performed using simultaneous thermal analysis unit (Jupiter STA 449 F3, Ceramic Research Centre, Turkey). The physical and mechanical properties such as water absorption, firing shrinkage, and bending strength were performed in Ceramic Research Centre in Eskisehir. According to ISO 13006 and EN 14441, the initial length of the green bodies was measured to determine the firing shrinkage. Then, green bodies were sintered at 1130 °C. Finally, the final length of the bodies was measured. The formula for the calculation of firing shrinkage is given below [8].

$$\%\ \text{Firing shrinkage} = \frac{(\text{Dry length} - \text{Fired length}) * 100}{\text{Dry length}}. \tag{1}$$

The fired samples were used to determine the water absorptions. Initially, the dry weight of the samples was measured (W_0). Then, the samples were taken into the hot water tank after they were kept in cold water for approximately 10 h. After 17 h in this tank, the final weights were measured (W_1) [6].

$$\%\ \text{Water absorption} = \frac{(W_1 - W_0) * 100}{W_1}. \tag{2}$$

According to the Archimedes principle, the bulk densities of the samples were calculated using Eq. 3 [8].

$$\text{Bulk density} = \left(\frac{W_0}{W_1 - W_2}\right) x \rho_{H_2O}. \tag{3}$$

W_2: suspended weight (g).

The bending strength and dry strength of the bodies were determined using 3-point bending strength method. The bending strength values were calculated using Eq. 4 [8].

$$\sigma = \frac{3FL}{2bd^2}. \tag{4}$$

F: load (N), L: the length of the support span (mm), b: width (mm), d: thickness (mm).

Experimental studies

Chemical analysis and batch compositions

Table 1 shows the raw materials' chemical analyses. According to the results of chemical analysis, the cement raw mix dust contained SiO_2, Al_2O_3, and high CaO. In this study, marble powder was used instead of calcite as a source of $CaCO_3$. The marble powder contained approximately 54% CaO and 0.71% SiO_2 (by weight). The fire loss

of the marble powder used was 43%. Table 2 shows the batch ratios of the compositions. While STD body contains kaolin, clay, quartz, sodium feldspar and calcite, CRMD and marble dust were used in RMD1 in a ratio of 2% and 9% instead of calcite, respectively. CRMD and marble dust were also used in RMD2 body in a ratio of 3% and 8% instead of calcite, respectively. CRMD and marble dust were used in RMD3 body in a ratio of 5% and 6%, respectively. In RMD4 body, CRMD and marble dust were used in a ratio of 10% and 1%, respectively.

Phase analysis (XRD)

Figure 1 provides the X-ray diffraction patterns of the samples. According to the XRD patterns, mullite, anorthite phases were formed in all bodies. Quartz was detected as a residual phase. The Anorthite and Mullite phases in RMD1, RMD2 and RMD3 increased with the addition of CRMD compared to the STD sample. This shows an increase in the anorthite phase affects physical and mechanical properties, such as bending strength [1, 2, 5–7]. The amount of anorthite phase in the RMD4 body decreased compared to the STD

Table 1 Chemical analyses (% by weight)

Raw materials	SiO_2	Al_2O_3	Fe_2O_3	TiO_2	CaO	MgO	Na_2O	K_2O	Lol
Kaolin	65.0	23.0	0.50	0.50	0.20	0.15	0.20	0.30	10.0
Sodium feldspar	71.10	17.40	0.05	0.24	0.60	0.10	9.36	0.34	0.50
Quartz	97.64	0.73	0.18	0.03	0.10	0.01	0.01	0.470	0.43
Marble dust	0.71	0.33	0.10	–	54.75	0.34	–	–	43.67
Clay	59.0	25.00	1.00	1.50	0.60	0.70	0.60	2.70	8.50
Cement raw mix dust	13.51	3.46	1.87	0.35	43.62	0.98	0.08	0.6	35.11
Calcite	0.7	0.29	0.03	–	54.8	1.0	0.04	0.08	43.5

LoI loss of ignition

Table 2 Batch ratios of the STD, RMD1, RMD2, RMD3 and RMD4 bodies

% By weight	Kaolin (%)	Clay (%)	Quartz (%)	Sodium feldspar (%)	Marble dust (%)	Calcite	CRMD (%)
STD	30	37	6	16	–	11	–
RMD1	30	37	6	16	9	–	2
RMD2	30	37	6	16	8	–	3
RMD3	30	37	6	16	6	–	5
RMD4	30	37	6	16	1	–	10

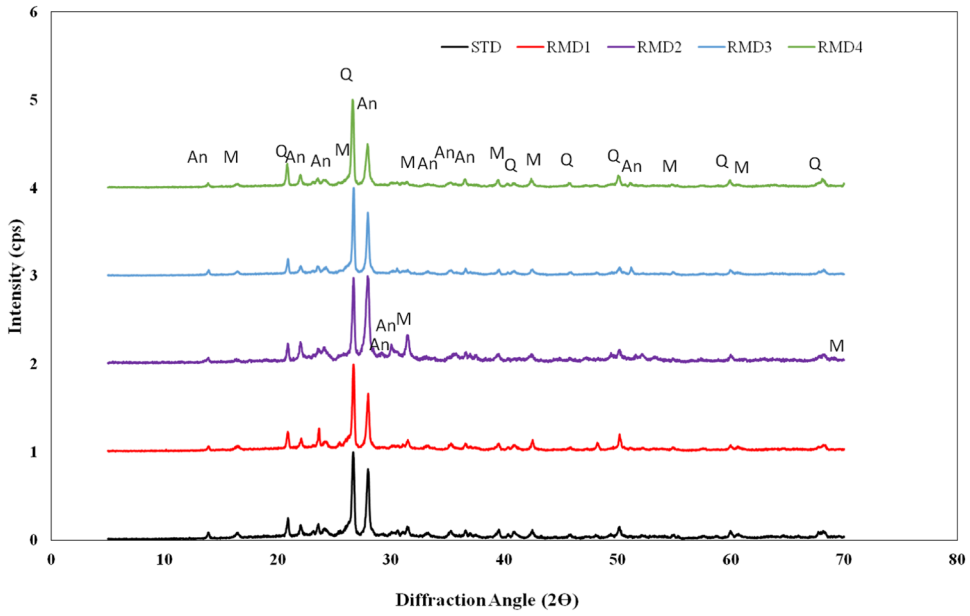

Fig. 1 X-ray diffraction patterns of the samples. An: anorthite, M: Mullite, Q: Quartz

body. This shows that the addition of a high percentage (5%) of cement waste raw mix dust adversely affects firing conditions [1]. Phase analysis shown that the main crystalline phase is anorthite phase, which is responsible for developing the strength of the samples. The anorthite phase was determined at a relatively high amount in the RMD1, RMD2 and RMD4 bodies. Anorthite was used commonly in ceramic tile industry due to its low sintering temperature and higher mechanical strength [6]. Thanks to the CRMD reacted with the liquid phase to form anorthite, it contributed to a higher mechanical strength in Sect. 3.3.

Physical and mechanical properties

Mullite morphology, mullite content, porosity, second phase formation, bulk density, etc. effect physical and mechanical properties of porcelain tile bodies. In ceramic wall tile bodies, their microstructure, physical and mechanical properties differ from those of porcelain tile bodies due to the higher porosity, low mullite content and smaller glassy phase content. Table 3 shows physical and mechanical properties such as bulk density, water absorption, firing shrinkage, dry strength, bending strength and colour measurement. The dry strength of the all samples increased with the addition of CRMD compared to the STD body. Bulk densities, bending strength increased in RMD1, RMD2, and RMD3 compared to the STD body with the addition of CRMD while water absorptions values decreased. The reason for this increase, which can be seen from the XRD graph, in the strength values is the increase in the amount of anorthite and mullite phases [1, 2, 5]. However, there was a decrease in RMD4 compared to the STD body. The addition of a high proportion (5%) of cement raw mix waste dust reduced the formation of anorthite and mullite phases, as it adversely affected the firing conditions. A previous study has shown this effect [1]. As a result of the decrease of the two main strength phases, the strength in the RMD4 body decreased. However, the decrease in strength in RMD4 is negligible. Because, according to ISO 13006 and EN 14441 standards, the minimum bending strength requirements for ceramic wall tiles is 152 kg/cm^2. Dry strength is an important production parameter for ceramic wall tiles to remain unbreakable during transport from one production line to another. Because ceramic wall tile bodies have higher amount of pores than the other ceramic tiles such as floor tile and porcelain tile. The higher amount of pores causes some production problems such as breakage and fragmentation. As seen in Table 3, the addition of CRMD allowed a 50% increase in dry strengths. This is the most remarkable result in this study. The higher dry strength contributes to increase the higher production stability and efficiency. The CIElab method was used for the color analysis [9–11]. Figure 2 provides images of the samples. According to this method, three main parameters were used to determine tile whiteness and color. The L * parameter refers to brightness;

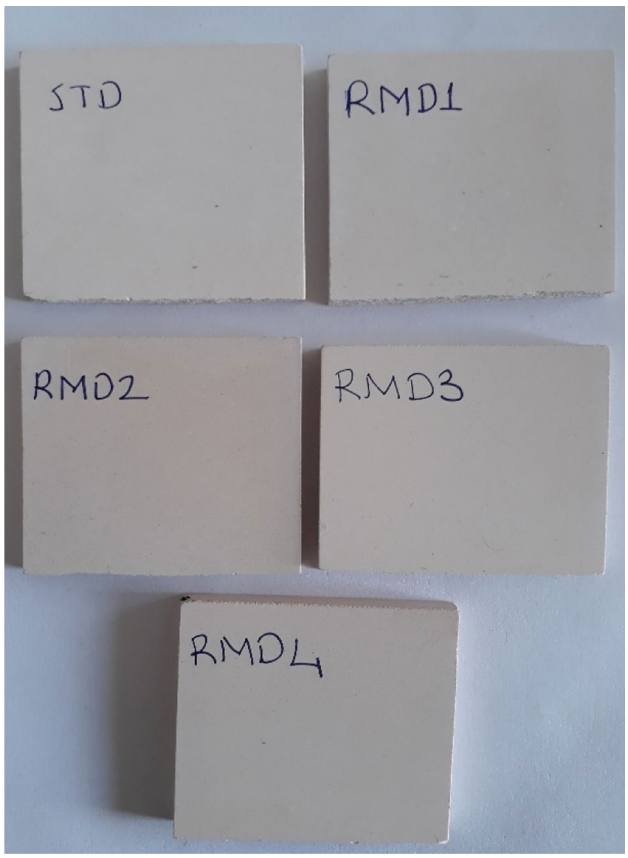

Fig. 2 Images of samples fired at 1130 °C

Table 3 Physical and mechanical properties

Sample	Bulk density (g cm^{-3})	Water absorption (%)	Firing shrinkage (%)	Dry strength (kg cm^{-2})	Bending strength (kg cm^{-2})	color measurement		
						L^*	a^*	b^*
STD	1.68	18.38	1.16	11.01	159.23	89.37	2.00	7.43
RMD1	1.72	17.66	1.40	16.62	174.13	89.32	2.01	7.28
RMD2	1.77	16.59	1.10	16.05	179.66	85.48	2.45	9.85
RMD3	1.75	18.07	0.58	16.93	161.96	88.08	2.43	9.20
RMD4	1.65	19.43	0.6	15.34	155.2	86.34	3.28	11.01

$L = 100$ means full whiteness, and $L = 0$ means full black. The a * parameter refers to the red–green color range, and the b * parameter refers to the yellow–blue color range [10, 11]. According to the data obtained in this study, the addition of CRMD precipitated a slight decrease in the whiteness value of the samples and a slight increase in the red and yellow color According to the literature, the increase in the amount of anorthite crystals contributes to an increase in the whiteness values of the ceramic bodies due to the opacifying effect [10]. However, high iron content of waste raw powder prevented increase of whiteness value.

TG–DTA

Figure 3 shows the thermal behavior of CRMD to investigate the phase evolution and the reaction mechanism. For cement raw mix waste dust, a pronounced endothermic peak at 855.7 °C in the DTA curve is due to the decomposition of CaCO3 [11, 12]. TG–DTG curves can explain this endothermic peak presented between 800 and 1000 °C. The mass loss is observed on the TG–DTG curves. The first mass loss, about 1.3 wt% at 70.2 °C, is attributed to the removal of moisture from the clay. The mass loss, about 1.36 wt%, is

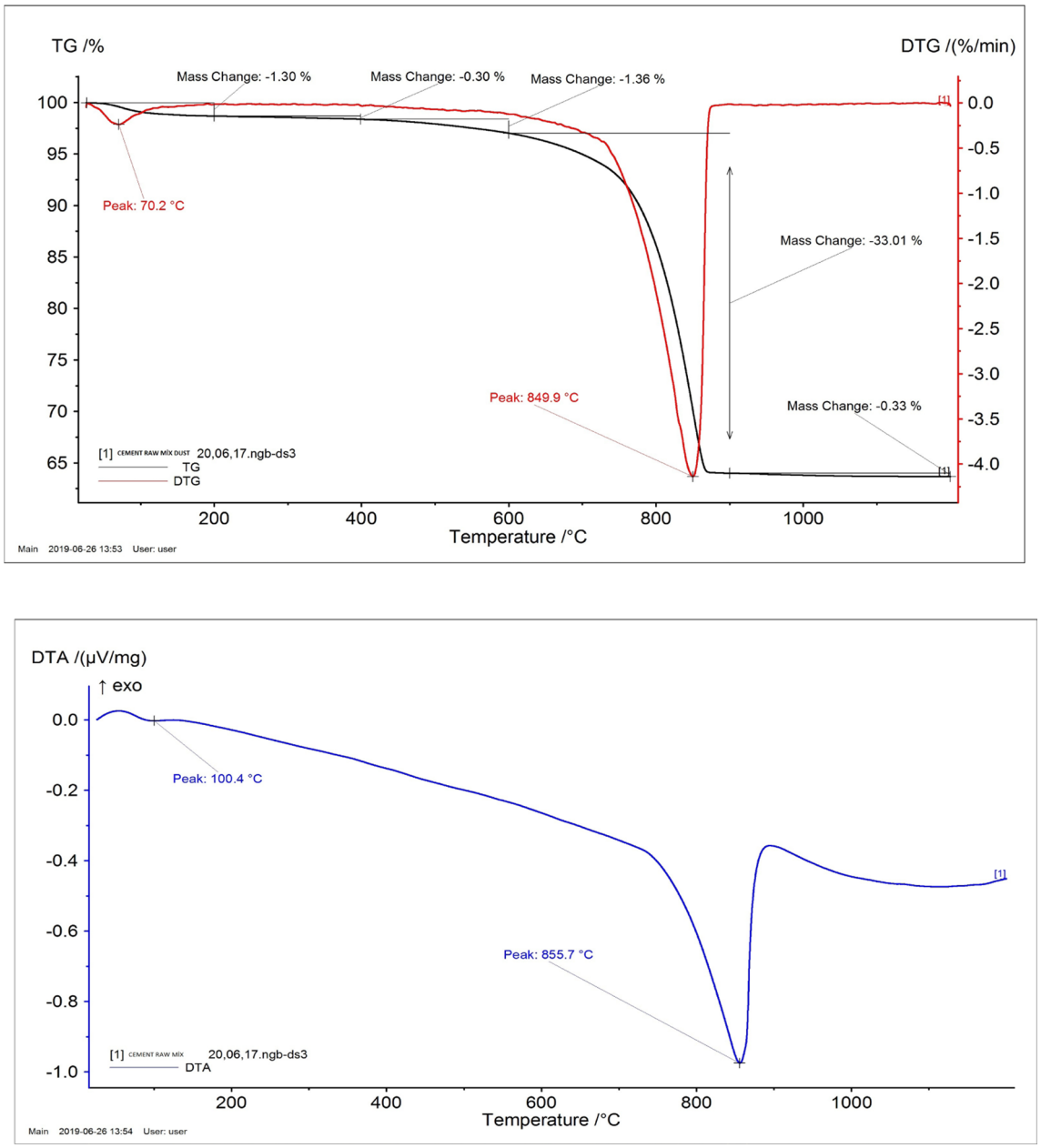

Fig. 3 TG–DTA graphs of CRMD

attributed to the removal of structural hydroxyls from the clay mineral at a temperature range of 400–600 °C. The third mass loss, about 33.1 wt%, for cement raw mix dust from 800 to 1000 °C is due to the decomposition of CaCO3 [13].

Optical dilatometer (sintering behavior)

Figures 4, 5 and 6 provide the results of firing analysis made with a non-contact optical dilatometer device. When examining the firing analysis curve of non-contact optical dilatometer of the STD wall tile in Fig. 4, the STD body was determined to exhibit rapid expansion up to about 600 °C. This is due to the quartz content of the marble powder. As known, quartz inversion is alpha and beta forms at 573 °C [12–15]. The expansion continued more slowly up to about 900 °C. Densification began after 900 °C [16]. The shrinkage was observed due to the metakaolinite transforms to a spinel-type phase and mullite (3Al2O3·2SiO2). The spinel-type phase can be Al-Si spinel or γ-Al2O3 (Al-spinel) [17]. However, it is difficult to say which type it is due to its small poor crystallinity and crystal size. The STD body crystalizes at 1039 °C. This crystallization resulted from the formation of anorthite. The decomposition of CaCO3 to CaO and CO2 takes place first [1, 2]. And then anorthite crystal forms from CaO and SiO2 between 1000 and 1050 °C. In Fig. 5, an examination of the firing analysis curves of CRMD determines that the RMD1 body exhibited similar behavior to the STD body. As the amount of CRMD increased, expansion and crystallization increased for RMD1 and RMD2. However, as Table 4 shows, the sintering rate (dy/dt) was negatively affected, and sintering slowed down (decrease in densification rate) for RMD3 and RMD4. The XRD analysis and technical properties supported this situation. As Table 4 shows, with the slowing down in the sintering rate (dy/dt), the crystallization and technical properties of RMD3 and RMD4 decreased. There are several theories to explain the mechanical properties of ceramic materials. Especially, some factors such as the content and morphology of mullite crystals and also quartz particles and porosity [18]. Thus, the strength of bodies increases with increasing mullite content. In this study, the strength of RMD1 and RMD2 increased due to the increase in crystallization of mullite and anorthite. However, in RMD3 and RMD4 bodies, the decrease in content of mullite anorthite and decrease in densification rate resulted in a decrease in strength values.

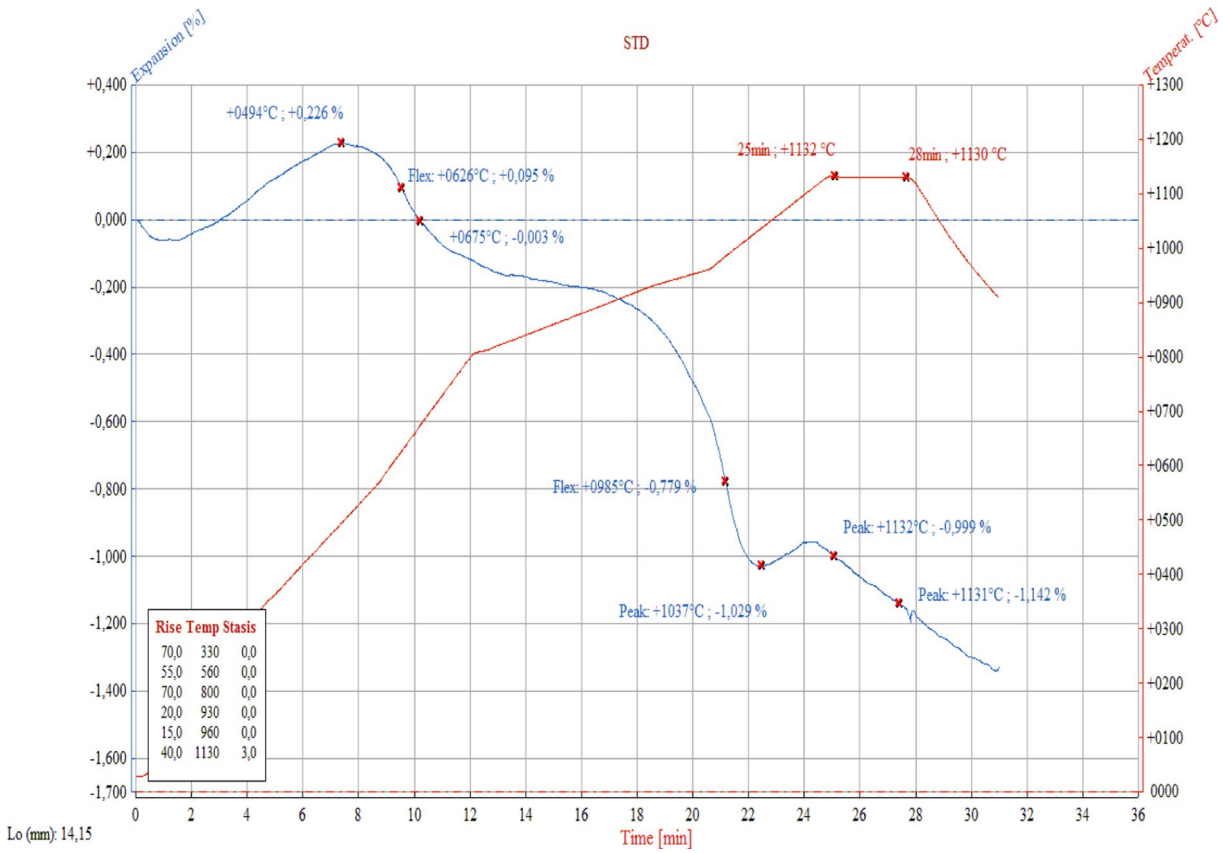

Fig. 4 Non-contact optical dilatometric sintering curve of the STD body

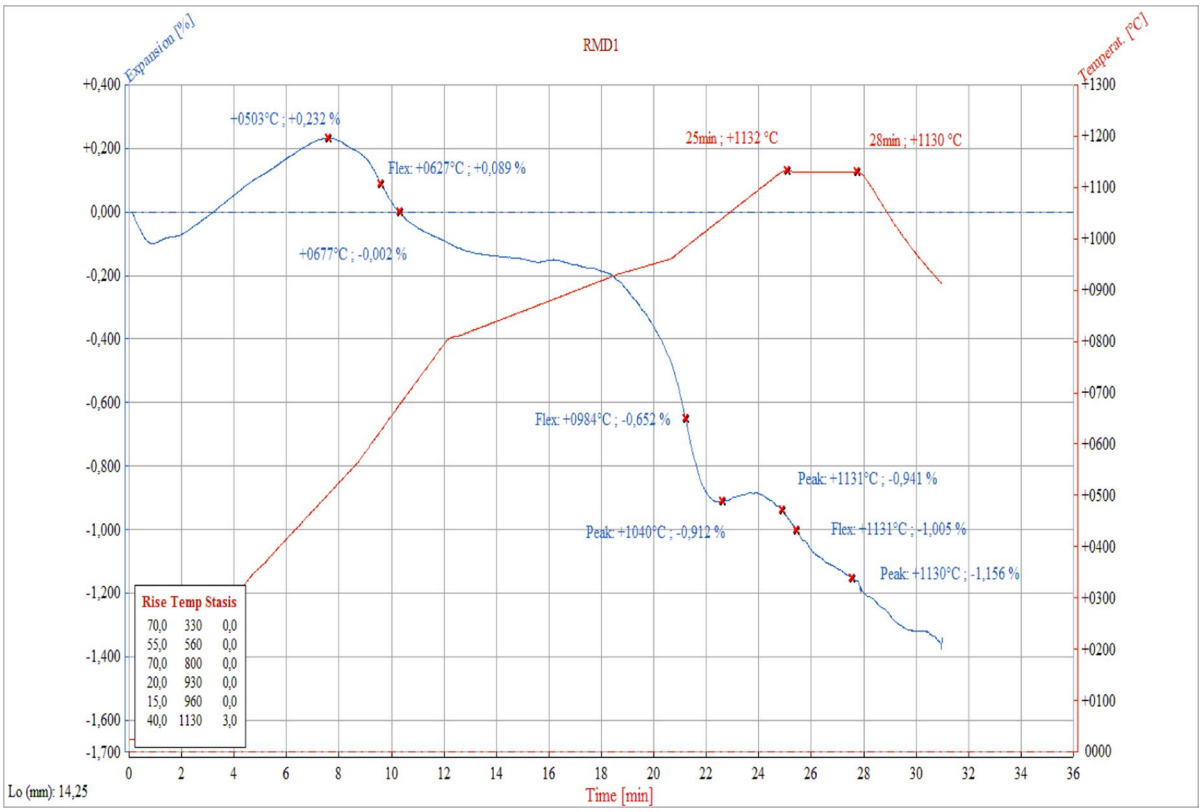

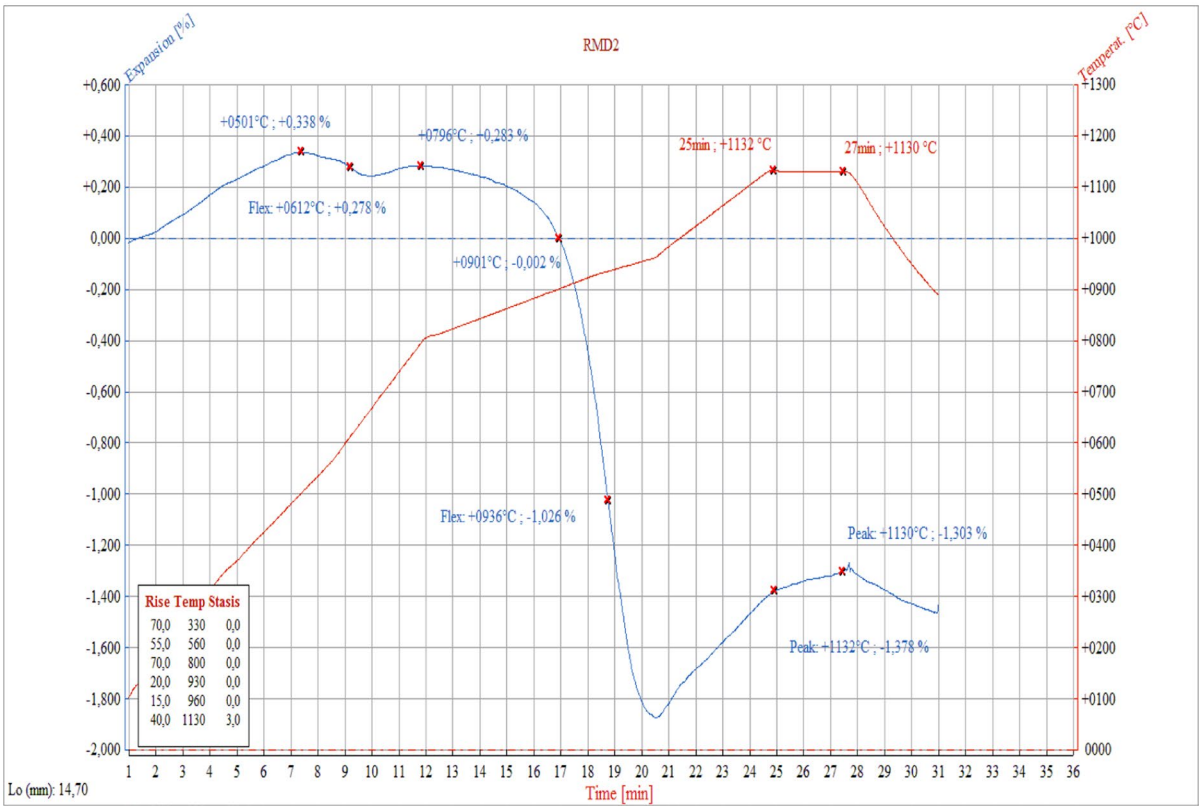

Fig. 5 Non-contact optical dilatometric sintering curves of RMD1 and RMD2

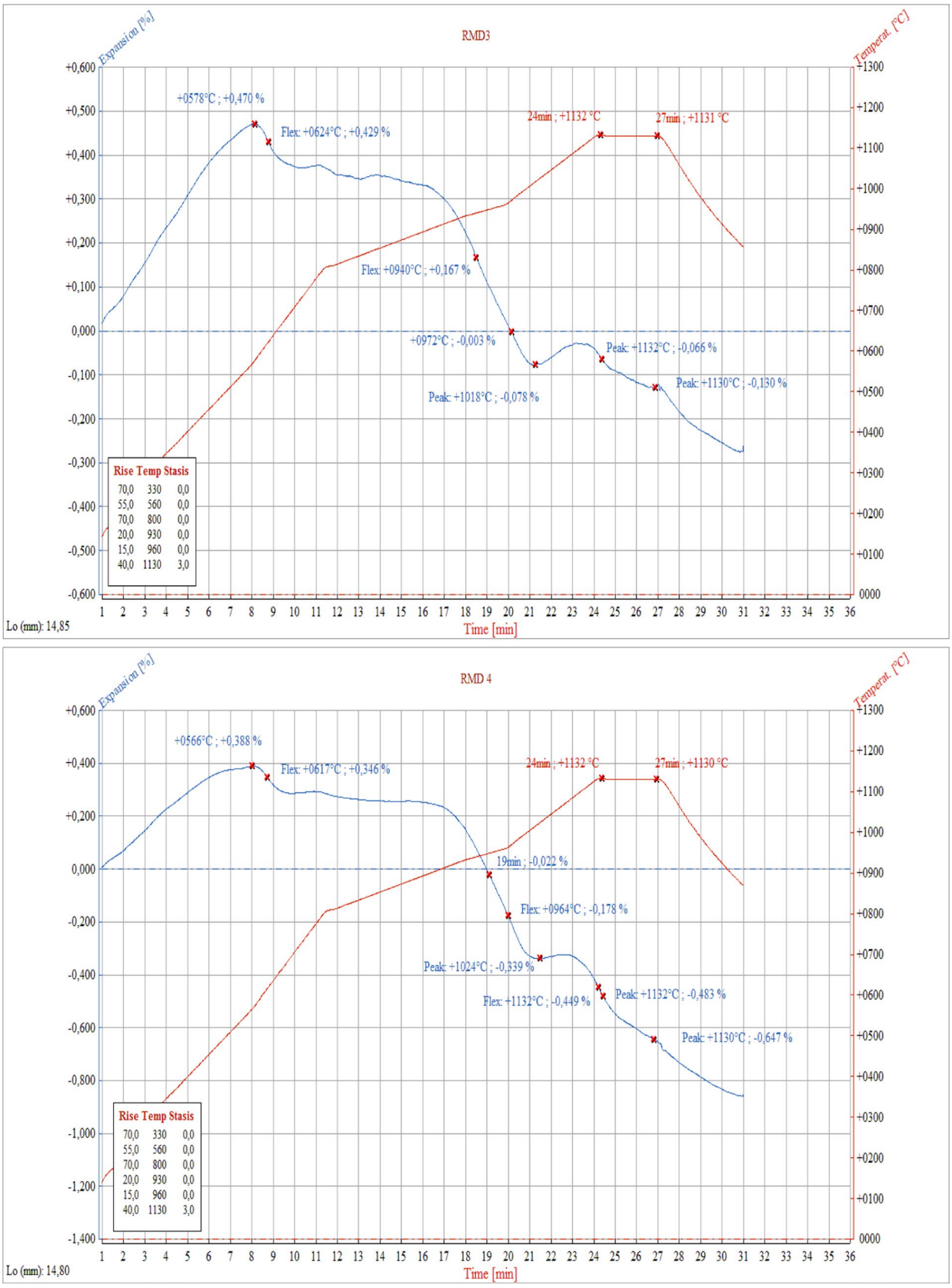

Fig. 6 Non-contact optical dilatometric sintering curves of RMD3 and RMD4

Table 4 Sintering rate (d*y*/d*t*) values of the STD, RMD1, RMD2, RMD3 and RMD4 bodies

	$dy/dt. 10^{-3}$
STD	5.691
RMD1	5.634
RMD2	13.59
RMD3	3.075
RMD4	1.87

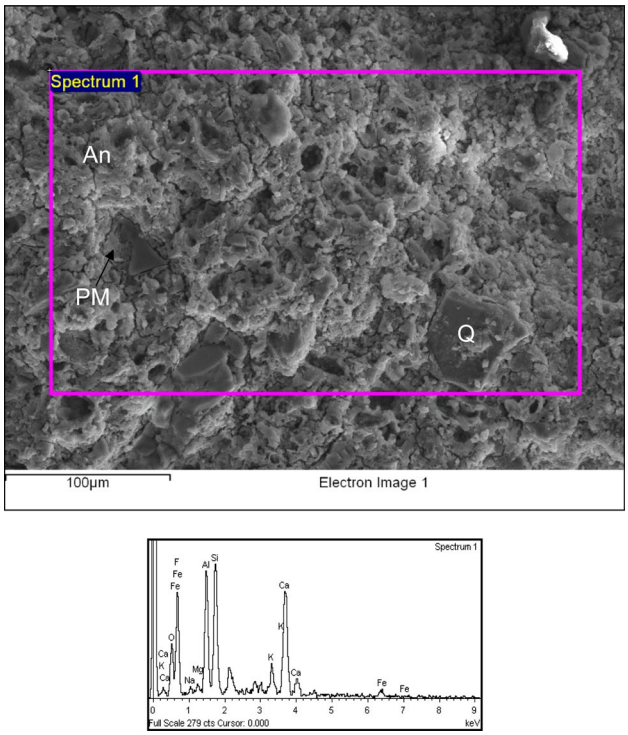

Fig. 7 Microstructure and EDX peaks of STD body. Q: quartz, An: anorthite, PM: primary mullite

Microstructural analysis (SEM–EDX)

SEM and EDX analyses were performed to show the relationship between microstructure, physical, mechanical and thermal properties of the samples. The microstructure images of the bodies are shown in Figs. 7, 8, 9, 10, 11. The EDX analyses of the samples are given in Table 5. The secondary electrons were used to detect the microstructure analysis. In Figs.7 and 9, the samples were investigated using line scan EDX method. In Figs. 8, 10, and 11, samples were investigated using spectral point EDX analysis. Figure 7 shows SEM analysis and EDX peaks of the STD body. According to SEM image and EDX peaks, quartz, primary mullite and anorthite crystals were detected. Anorthite crystals (CaAl2Si2O8) were formed from CaCO3 calcination during the thermal cycle to CaO and CO2 [1, 2, 6]. Primary mullite crystal (3Al2O32SiO2) forms from metakaolin and

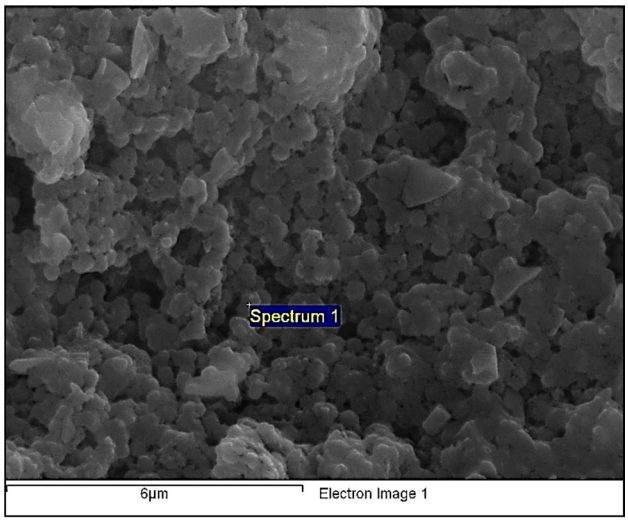

Fig. 8 Microstructure and EDX peaks of RMD1 body

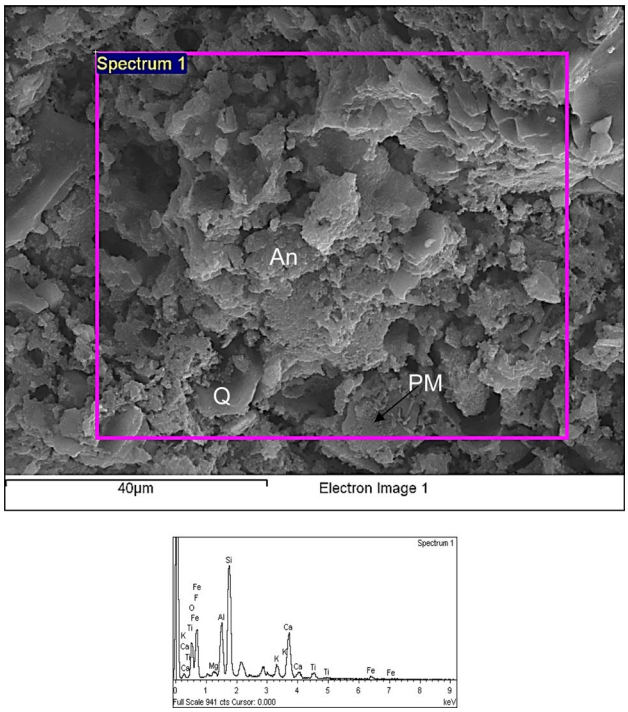

Fig. 9 Microstructure and EDX peaks of RMD2 body. Q: Quartz, An: Anorthite, PM: Primary mullite

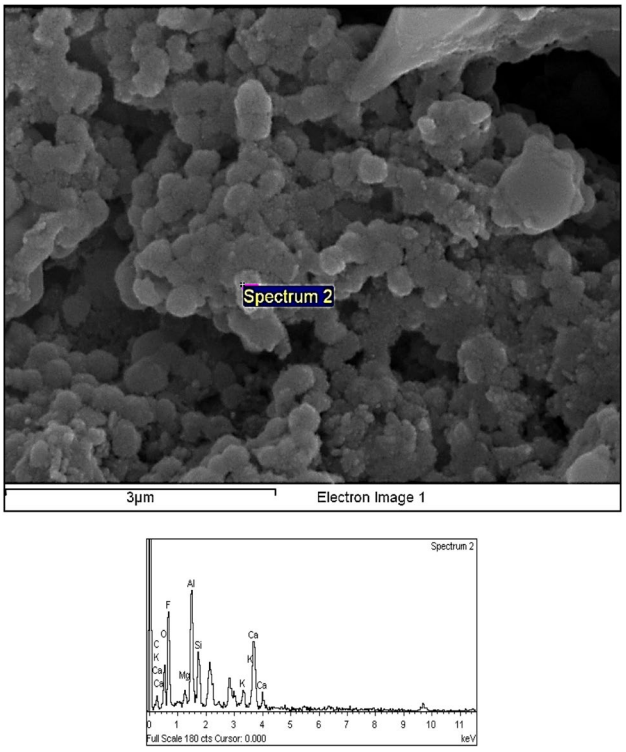

Fig. 10 Microstructure and EDX peaks of RMD3 body

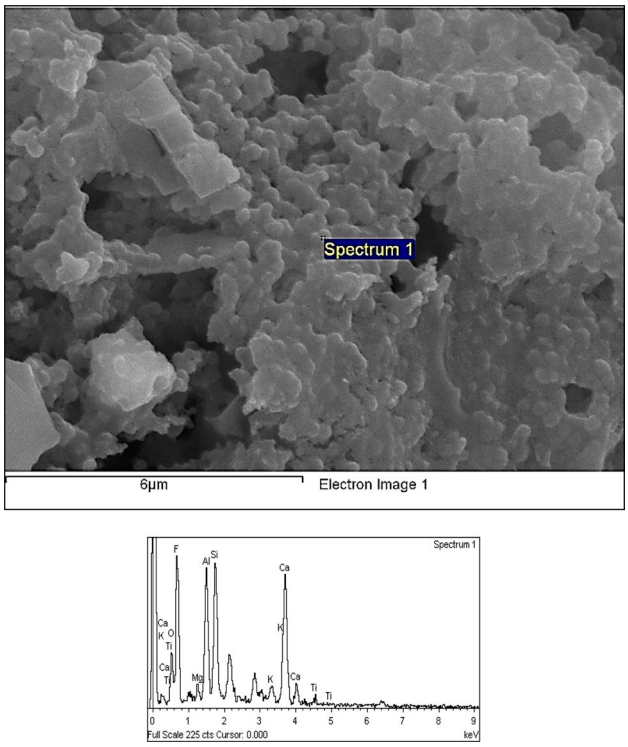

Fig. 11 Microstructure and EDX peaks of RMD4 body

Table 5 EDX analysis of bodies

Element	Weight%	Atomic%	Compound%	Formula
STD				
Na K	1.21	1.18	1.64	Na_2O
Mg K	1.05	0.96	1.73	MgO
Al K	13.53	11.24	25.57	Al_2O_3
Si K	17.34	13.83	37.09	SiO_2
K K	4.48	2.57	5.40	K_2O
Ca K	20.42	11.42	28.57	CaO
O	41.97	58.79		
Totals	100.00			
RMD1				
Al K	16.80	15.03	31.75	Al_2O_3
Si K	5.11	4.39	10.94	SiO_2
K K	2.10	1.29	2.53	K_2O
Ca K	36.59	22.03	51.20	CaO
Ti K	2.15	1.08	3.59	TiO_2
O	37.24	56.17		
Totals	100.00			
RMD2				
Mg K	0.89	0.80	1.47	MgO
Al K	9.75	7.91	18.42	Al_2O_3
Si K	24.35	18.97	52.08	SiO_2
K K	3.31	1.85	3.99	K_2O
Ca K	14.13	7.72	19.78	CaO
Ti K	2.56	1.17	4.27	TiO_2
O	45.02	61.58		
Totals	100.00			
RMD3				
Mg K	2.33	2.15	3.86	MgO
Al K	20.44	17.00	38.62	Al_2O_3
Si K	11.12	8.88	23.79	SiO_2
K K	4.35	2.49	5.24	K_2O
Ca K	20.36	11.40	28.49	CaO
O	41.40	58.07		
Totals	100.00			
RMD4				
Mg K	1.98	1.82	3.28	MgO
Al K	13.83	11.49	26.13	Al_2O_3
Si K	16.54	13.21	35.39	SiO_2
K K	2.48	1.42	2.98	K_2O
Ca K	21.27	11.90	29.76	CaO
Ti K	1.48	0.69	2.46	TiO_2
O	42.43	59.47		
Totals	100.00			

non-equilibrium unstable spinel-type phase. After metakaolin transforms to non-equilibrium unstable spinel-type phase, primary mullite crystals (cuboidal) start to form above 1075 °C [19]. The crystal phase regions containing anorthite are composed of SiO2, Al2O3, CaO and Na2O

and MgO in Table 5. Figure 8 shows the microstructure and EDX peaks of RMD1 body. Table 5 also shows the EDX analysis of RMD1 body. As seen on Fig. 8, anorthite crystals were detected. The EDX analysis in Table 5 confirmed that the crystals are anorthite crystals. The crystal phase regions containing anorthite are composed of SiO2, Al2O3, CaO and K2O and TiO2 in Table 5. The microstructure and EDX peaks of RMD2 body are given in Fig. 9. Densely formed anorthite crystals were observed. EDX peaks and EDX analysis in Fig. 9 and Table 5 confirmed that the crystals are anorthite crystals. The cuboidal-shaped mullite crystals (primary mullite) were also detected. Figure 10 shows microstructure and EDX peaks of RMD3 body. EDX analysis of RMD3 body is also given in Table 5. As seen on Fig. 10, anorthite crystals were detected. The crystal phase regions containing anorthite are composed of SiO2, Al2O3, CaO, K2O and MgO in Table 5. As seen on Fig. 11, anorthite crystals were detected in RMD4 body. The crystal phase regions containing anorthite are composed of SiO2, Al2O3, CaO and K2O, MgO and TiO2 in Table 5.

Especially, as seen on Figs. 10 and 11, decrease in densification rate resulted in a decrease in mullite content in RMD3 and RMD4. This result was responsible for decrease in bending strength of RMD3 compared to RMD1 and RMD2. However, bending strength of RMD3 is still higher than STD due to the higher amount of anorthite formation. Decrease in densification rate due to the high amount of CRMD addition also caused a decrease in bending strength of RMD4 body compared to other bodies. However, densely formed anorthite crystals also contributed to the bending strength values of RMD4 within the standard values in spite of the decrease in mullite content.

Conclusion

The study used a cement raw mixed waste dust (max 10% by weight) in a standard ceramic wall tile composition as a source of $CaCO_3$. Crystalline phases such as mullite and anorthite in RMD1, RMD2, and RMD3 increased with the addition of CRMD compared with STD body. The addition of waste dust positively affects technological properties such as bending strength, dry strength, and bulk density. The addition of waste dust greater than 5% by weight negatively affects technological properties. This is, however, negligible. Because the bending strength values are still within the standards (ISO 13006 and EN 14441). More importantly, dry strength is one of the most important properties of ceramic tiles during production. In this study, it was shown that 50% increase in dry densities was achieved with the addition of CRMD. This is important due to production stability and efficiency. The most important difference that distinguishes this study from previous studies is the increase in dry strengths. Although the use of a high percentage of CRMD and marble dust (5% and over) adversely affected the sintering rate, physical and mechanical properties are still in ISO 13006 and EN 14441 standards. So CRMD can be used as an alternative source of raw material since it improves many technical features in ceramic tiles.

Acknowledgements I would like to thank the Ceramics Research Center, Eskisehir, Turkey and Aslan Cement Co., Kocaeli, Turkey for their support in this work.

References

1. Aydin T, Paksoy C (2019) The effect of cement raw mix waste dust on porcelain tile properties. J Aust Ceram Soc 55:37–45
2. Aydin T, Tarhan M, Tarhan B (2019) Addition of cement kiln dust in ceramic wall tile bodies. J Therm Anal Calorim 136:527–533
3. Devi KS, Lakshmi VV, Alakanandana A (2017) Impacts of cement industry on environment—an overview Asia Pacific. J Res. I. LVII:156–161
4. Mishra S, Siddiqui NA (2014) A review on environmental and health ımpacts of cement manufacturing emissions. Int J Geol Agric Environ Sci 2:26–31
5. Tarhan M, Tarhan B, Aydin T (2016) The effects of fine fire clay sanitaryware wastes on ceramic wall tiles. Ceram Int 42:17110–17115
6. Ozturk ZB, Eren E (2015) Preparation of ceramic wall tiling derived from blast furnace slag. Ceram Int 41(9):12020–12026
7. Aydin T (2018) Investigation of the effects of blast furnace slag on ceramic sanitaryware bodies. Int J Eng Res Dev 10:178–182
8. Aydın T (2012) Investigation of stain resistance of porcelain tiles doped by spodumene. (Ph.D. thesis), Anadolu University, Eskisehir, Turkey
9. https://cielab.xyz/pdf/cie.15.2004%20colorimetry.pdf, CIE international commission on illumination, Technical report, Colorimetry, ISBN 3 901 906 33 9
10. Tarhan M (2019) Whiteness improvement of porcelain tiles incorporated with anorthite and diopside phases. J Therm Anal Calorim. https://doi.org/10.1007/s10973-019-08268-8
11. Selli NT (2015) Development of anorthite based white porcelain stoneware tile compositions. Ceram Int 41:7790–7795
12. Sousa SJG, Holanda JNF (2005) Sintering behavior of porous wall tile bodies during fast single-firing process. Mater Res 8:197–200
13. Ke S, Cheng X, Wang Y, Wang Q, Wang H (2013) Dolomite, wollastonite and calcite as different CaO sources in anorthite-based porcelain. Ceramics Int 39:4953–4960
14. Lu J, Li Y, Zou C, Liu Z, Wang C (2019) Effect of heating rate on the sinterability, crystallization, and mechanical properties of sintered glass–ceramics from granite waste. J Therm Anal Calorim 135:1977–1985
15. Hulan T, Trnik A, Kaljuvee T, Uibu M, Stubna I, Kallavus U, Traksmaa R (2017) The study of firing of a ceramic body made from illite and fluidized bed combustion fly ash. J Therm Anal Calorim 127:79–89
16. Hossain SK, Ranjan V, Pyare R, Roy PK (2019) Study the effect of physico-mechanical characteristics of ceramic tiles after addition of river silts and wollastonite derived from wastes. Constr Build Mater 209:315–325
17. Lee S, Kim YJ, Moon HS (1999) Phase transformation sequence from kaolinite to mullite investigated by an energy-filtering transmission electron microscope. J Am Ceram Soc 82(10):2841–2848

18. Márquez JM, Rincón JM, Romero M (2010) Effect of microstructure on mechanical properties of porcelain stoneware. J Eur Ceram Soc 30:3063–3069
19. Mustafi S, Ahsan M, Dewan AH, Ahmed S, Khatun N, Absar N (2011) Effect of waste glass powder on physico-mechanical properties of ceramic tiles. Bangladesh J Sci Res 24(2):169–180